Clinical Neurophysiology 124 (2013) 228–237

Contents lists available at SciVerse ScienceDirect

Clinical Neurophysiology

journal homepage: www.elsevier.com/locate/clinph

Quantification of the adult EEG background pattern

Shaun S. Lodder [a,*], Michel J.A.M. van Putten [a,b,*]

[a] Clinical Neurophysiology, MIRA-Institute for Biomedical Technology and Technical Medicine, University of Twente, The Netherlands
[b] Department of Neurology and Clinical Neurophysiology, Medisch Spectrum Twente, Enschede, The Netherlands

ARTICLE INFO

Article history:
Accepted 14 July 2012
Available online 20 August 2012

Keywords:
Quantitative EEG analysis
Automated interpretation
Background pattern
Guidelines
Inter-rater reliability

HIGHLIGHTS

- We attempt to quantify the same background properties reported by routine visual analysis, and in addition, compare the quantitative output to that of the human reviewer.
- Five properties are quantified: alpha rhythm frequency, reactivity, anterio–posterior gradients, asymmetries, and diffuse slow-wave activity.
- Quantitative analysis as an assistive tool can improve consistency and inter-rater reliability in reporting of the EEG background pattern.

ABSTRACT

Objective: Visual interpretation of EEG is time-consuming and not always consistent between reviewers. Our objective is to improve this by introducing guidelines and algorithms to quantify various properties, focussing on the background pattern in adult EEGs.
Methods: Five common properties were evaluated: (i) alpha rhythm frequency; (ii) reactivity; (iii) anterio–posterior gradients; (iv) asymmetries; and (v) diffuse slow-wave activity. A formal description was found for each together with a guideline and proposed quantitative algorithm. All five features were automatically extracted from routine EEG recordings. Modified time-frequency plots were calculated to summarize spectral and spatial characteristics. Visual analysis scores were obtained from diagnostic reports.
Results: Automated feature extraction was applied to 384 routine EEGs. Inter-rater agreement was calculated between visual and quantitative analysis using Fleiss' kappa: $\kappa = \{$(i) 0.60; (ii) 0.35; (iii) 0.19; (iv) 0.12; (v) 0.76$\}$. The method is further illustrated with three representative examples of automated reports.
Conclusions: Automated feature extraction of several background EEG properties seems feasible. Inter-rater agreement differed between various features, ranging from slight to substantial. This may be related to the nature of various guidelines and inconsistencies in visual interpretation.
Significance: Formal descriptions, standardized terminology, and quantitative analysis may improve inter-rater reliability in reporting of the EEG background pattern and contribute to more efficient and consistent interpretations.

1. Introduction

For almost a century the electroencephalogram (EEG) has been an important and invaluable technique in clinical neurology. Applications include the differential diagnosis of developmental disorders, sleep analysis, and the diagnostic process in epilepsy. Despite tremendous advances in computing power and the availability of digital recordings, the gold standard for the interpretation is still visual analysis. Perhaps the very large variability in EEG patterns, both in physiological and in pathological conditions, limit efforts to automate the diagnostic process. At the same time, the human brain is an expert in visual analysis, including the rejection of artefacts and detection of transients. The processes involved are indeed not trivial to replace by computer analysis (Halford, 2009).

In general, EEG analysis in clinical neurology consists of two parts: analysis of the background pattern and detection of transients (Schomer and Lopes da Silva, 2010; van Putten, 2009). The background pattern can be defined as the mean statistical charac-

* Corresponding authors. Address: Department of Clinical Neurophysiology, Building Carre, Science and Technology, P.O. Box 217, 7500 AE Enschede, The Netherlands. Tel.: +31 53 489 4599.
E-mail addresses: S.S.Lodder@utwente.nl (S.S. Lodder), M.J.A.M.vanPutten@utwente.nl (M.J.A.M. van Putten).

1388-2457/$36.00
http://dx.doi.org/10.1016/j.clinph.2012.07.007

teristics of the EEG, and includes features such as the posterior dominant rhythm, reactivity, frequency distribution over the scalp, and the presence or absence of asymmetries. Transients refer to relatively rare events, and include both physiological and pathological waveforms, such as lambda waves, wicket waves or spike-wave discharges.

An accurate interpretation of both the background pattern and the transients is of high importance for correct diagnostics. Unfortunately, various studies have shown that a large inter- and intra-observer variability still exists between reviewers. Depending on the reported feature or decision outcome, the inter-rater agreement (Kappa coefficients) range from slight (0.09) to substantial (0.94) (Haut et al., 2002; Benbadis et al., 2009; Gerber et al., 2008; Azuma et al., 2003). One of the main reasons for this is a lack of consistency in describing the properties accurately. Azuma et al. (2003) showed that by conforming to a set of general guidelines, inter-rater variability could be reduced significantly (Azuma et al., 2003). For many of the EEG properties mentioned however, formal guidelines do not exist or fall short of being used. In addition to this, EEG reports lack consistent terminology to describe the severity of an abnormality.

Apart from improving inter-rater reliability in reports, possibilities exist with computational methods to increase reviewer efficiency and to find characteristics that are hard or even impossible to detect by visual analysis alone. Substantial progress has been made with quantitative methods in the fields of seizure and spike detection (van Putten, 2003; van Putten et al., 2005; Kurtz et al., 2009; Halford, 2009; Wilson and Emerson, 2002), but little exists for describing the EEG background pattern quantitatively. Given that background properties provide essential information to the clinician, the use of quantitative tools may be advantageous in assisting with the analysis.

In this paper, we address two issues related to the reviewing of EEGs in a clinical environment. First, we propose guidelines for describing background properties to improve consistency and reduce inter-rater variability. Secondly, by building methods around these guidelines, we introduce quantitative algorithms to measure five of the most commonly reported background properties. The guidelines are kept simple (but feasible) to maximize consensus between reviewers, and the quantitative values are designed intuitively to allow for interpretation in a useful manner. We evaluate our work by comparing reports generated with the quantitative techniques against EEG reports from visual interpretation, and also show two examples where quantitative analysis is used to identify abnormal background patterns.

2. Methods

2.1. Data

The dataset for this study was obtained from the department of Clinical Neurophysiology of the Medisch Spectrum Twente (MST). The recordings were made over a period of five years, and for each EEG a standard 20–30 minute recording protocol was used. Electrode impedances were kept below 5 kΩ to reduce polarization effects, and standard EEG caps were used with 19 Ag–AgCl electrodes placed according to the international 10–20 system. The recordings were made at a sample rate of 250 Hz using a common reference (Brainlab, OSG BVBA). Technicians annotated eyes open, eyes closed, hyperventillation and photic stimulation events during all recordings.

From the MST database, we selected recordings that were originally made as part of epilepsy investigations. A total of 384 records were used for evaluation, and the patient group consisted of 214 males and 170 females with ages ranging from 18 to 90 years.

Table 1
Summary of EEGs described by visual analysis. Descriptions obtained from diagnostic reports.

Alpha rhythm peak frequency		
Normal for age		Deviating from norm
303 (90%)		33 (10%)
Reactivity		
Substantial	Moderate	Low or absent
301 (90%)	26 (8%)	9 (3%)
Anterio–posterior gradient		
Normal range	Moderate differentiation	Abnormal or deviant
286 (74%)	73 (19%)	25 (7%)
Asymmetries		
None		At least one
295 (77%)		89 (23%)
Diffuse slow-wave activity		
Normal EEG patterns		Diffuse slow waves
347 (90%)		37 (10%)

For each recording, a diagnostic report written prior to the construction of the proposed guidelines was available. These reports were written by one of two board certified neurologists, and they were used to compare interpretations between visual- and quantitative analysis. In order to compare the interpretations, the free text reports were carefully read and all background properties were categorized by the authors based on a designated set of outcomes for each property. Recordings were excluded if their reports had missing information about any of the properties considered in this study. Table 1 shows the outcomes and summarizes the dataset as described by the reports.

2.2. Preprocessing

An independent component analysis filter was used to reduce the influence of eye blink artifacts on the described features. After calculating the independent components, each was compared to a electrooculogram (EOG) channel recorded together with the EEG. If one of the components showed a substantial correlation with the EOG channel (>0.3), it was removed by setting all its values to zero. The remaining components were projected back to their channel space by applying the inverse transform. No other artifact detection or reduction was performed.

2.3. EEG features

We focus on five common background properties: (i) the alpha rhythm[1] and its peak frequency; (ii) reactivity; (iii) anterio–posterior gradients; (iv) asymmetries; and (v) the presence or absence of diffuse slow-wave activity. Each of these properties is discussed in the subsections to follow. Other reported background properties include beta activity, lambda waves, changes during hyperventilation, and driving responses during photic stimulation. These properties were however not investigated.

Each subsection below starts with an outline of a property, followed by a proposed guideline to evaluate or describe it, and then followed by a quantitative analysis approach to evaluate the property in a computational manner. Depending on the quantitative feature calculated, either a common reference, Laplacian, or bi-polar montage was used. Annotations were extracted in an automated manner to determine eyes open and eyes closed states, and segments during hyperventilation and photic stimulation were ignored. Detailed descriptions of the quantitative algorithms are presented in Appendix A.

[1] A more general name is the posterior dominant rhythm, as in pathological situations the peak frequency may be outside the alpha frequency range. Here, we will further denote it as the alpha rhythm.

2.3.1. Alpha rhythm frequency

The alpha rhythm was the first rhythmic activity measured in the brain and has been shown to have diagnostic value in diseases ranging from depression (Segrave et al., 2010; Spronk et al., 2011) and schizophrenia (Knyazeva et al., 2008; Jin et al., 2006) to Alzheimer's disease (Ishii et al., 2010; Lee et al., 2010) and visual perception (Babiloni et al., 2006; Sewards and Sewards, 1999). The alpha rhythm is most visible over the posterior regions during a relaxed state of wakefulness when the eyes are closed, and its frequency follows a downward gradient from the posterior region anteriorly when measured over the scalp (Segalowitz et al., 2010). Its peak frequency increases with age until maturation is reached, which typically occurs during adolescence or young adulthood (van der Stelt, 2008; Marcuse et al., 2008; Segalowitz et al., 2010). Thereafter it remains constant, or in some cases, decreases slowly with ageing (Lodder and van Putten, 2011). Decreasing alpha rhythm frequencies with ageing have been suggested to relate to mental deterioration (Gaál et al., 2010).

In various handbooks, it is stated that a posterior dominant rhythm of less than 8 Hz during wakefulness in an adult is abnormal (Levin and Lüders, 2000). In healthy individuals, even in the seventh and eighth decade, the mean is maintained at or above 9 Hz (Obrist, 1976). In a previous study, we found this also to be true in a dataset of 1215 normal EEGs (Lodder and van Putten, 2011). For children however, alpha peak frequencies can be normal below 8 Hz.

Guideline 1: The alpha rhythm frequency is defined as the peak frequency in a spectrogram taken over the posterior region during the eyes-closed state. For a guideline to take age dependency of the peak frequency into account, we propose to use the mean trend over age for normal EEGs, as noted by van der Stelt (2008), Segalowitz et al. (2010), Aurlien et al. (2004), and Lodder and van Putten (2011). Table 2 provides a reference derived from the mean trend approximated by Lodder and van Putten (2011), and we consider the alpha rhythm to deviate from the norm (i.e., too slow or fast) if the peak frequency differs by more than 1.8 Hz from the reference value for a given age.

Automated analysis: To find the alpha rhythm frequency with an algorithmic approach, a method previously described in Lodder and van Putten (2011) is used (summarized in Appendix A.2). Using a common reference montage, the technique identifies dominant frequency components between 3 and 18 Hz in the occipital region. This is done by fitting a curve to the log spectrum of localized segments of the EEG when the eyes are closed:

$$P_{\log}(f) \approx P_{\mathrm{fit}}(f) = P_{\mathrm{pk1}}(f) + P_{\mathrm{pk2}}(f) + P_{\mathrm{bg}}(f) \quad (1)$$

Peak parameters from the localized segments are clustered together based on frequency similarity, and an alpha rhythm estimate is obtained by finding the mean frequency of the largest cluster. If there are no dominant peaks in the EEG spectra, the method assumes that an alpha rhythm is not present. After estimating the alpha rhythm peak frequencies, they are categorized using Guideline 1 and Table 2 as reference.

Table 2
Reference to accepted normal alpha rhythm peak frequencies over age. From 0 to 15 years, the peak frequency is strongly related to age.

Age	Frequency (Hz)
0–1 yrs	5.3 ± 1.8
2–3 yrs	6.8 ± 1.8
4–5 yrs	7.9 ± 1.8
6–7 yrs	8.7 ± 1.8
8–15 yrs	9.5 ± 1.8
16–50 yrs	9.9 ± 1.8
>51 yrs	9.1 ± 1.8

2.3.2. Alpha rhythm reactivity

Reactivity is known as an attenuation of rhythmic activity, occurring mostly in the alpha band, when the brain receives an external stimulus after an idle state (Schomer and Lopes da Silva, 2010). The stimulus can range from eyes opening to auditory input or pain. Reactivity becomes weaker during drowsiness as compared to a fully awake state, and the level of suppression varies with age (Gaál et al., 2010). Although having less diagnostic value than other background properties, the reactivity is known to be lower in demented patients (van der Hiele et al., 2007; Babiloni et al., 2010). Furthermore, it is believed that lower reactivity reflects a reduction of neuronal interconnectivity and a weaker level of neurotransmission, which may be seen in EEGs of the elderly (Gaál et al., 2010). In previous studies by Logi et al. (2011), Douglass et al. (2002), and Ramachandrannair et al. (2005), the prognostic value of reactivity in comatosed patients was also explored with positive results.

Although reactivity is most commonly associated with the suppression of alpha power, a formal definition to quantify it with a scale of normality was not found in existing literature. Most studies compare the alpha power in an idle state to that of a non-idle state, as done for example by van der Hiele et al. (2007), Könönen and Partanen (1993), and Partanen et al. (1997).

Guideline 2: To categorize reactivity, we compare the difference in alpha power over the occipital region between an idle (relaxed, eyes closed) and non-idle (eyes open) state. Suppression of more than 50% alpha power is considered substantial, between 10% and 50% as moderate, and anything less as low or absent.

Automated analysis: Using the alpha frequency obtained by the technique described in Section 2.3.1, reactivity is calculated by comparing the difference in alpha power between eyes-open and eyes-closed states. The states are determined by evaluating annotations in the EEG. Using a narrow band around the alpha rhythm peak frequency, reactivity is calculated as

$$Q_{\mathrm{REAC}} = 1 - \frac{P_{EO}}{P_{EC}}, \quad (2)$$

where P_{EO} is the mean occipital power in a 0.5 Hz frequency band when the eyes are open and P_{EC} the mean occipital power in that band when the eyes are closed. The reactivity is classified as substantial when $Q_{\mathrm{REAC}} > 0.5$, moderate for $0.1 < Q_{\mathrm{REAC}} < 0.5$, and low or absent if $Q_{\mathrm{REAC}} < 0.1$.

2.3.3. Alpha power anterio–posterior gradient

Rhythmic activity from a normal wake brain should be distributed with an anterior-to-posterior gradient over the scalp: higher frequency beta activity with low voltages more prominently over the frontal regions fading posteriorly, and slower waves (e.g., alpha and mu rhythm) with higher voltages over the parietal and occipital lobes (Schomer and Lopes da Silva, 2010). Drowsiness and sleep causes attenuation of the alpha rhythm and slowing of the background rhythm, together with more prominent alpha and theta activity anteriorly. Medication (e.g., benzodiazepines) and anaesthesia (e.g., propofol) can also play a large role in the distribution of rhythmic activity, making it important to evaluate the gradient within clinical context to avoid misinterpretation. Abnormalities in the gradient can point to disorders such as schizophrenia and dementia (Knyazeva et al., 2008; Stevens and Kircher, 1998).

In the EEG reports reviewed, the anterio–posterior gradient described was mainly on alpha band activity. To have clinical relevance, our proposed guideline therefore also focusses on the alpha power distribution.

Guideline 3: Using a Laplacian montage, the gradient is categorized as 'within normal range' if the alpha power distribution is most prominent over the posterior region, 'moderate differentia-

tion' when it becomes evenly distributed over the scalp, and 'abnormal or deviant' if more power is present anteriorly than posteriorly.

Automated analysis: Based on the *center-of-gravity* feature in van Putten (2008), the mean power in the alpha band during an eyes-closed state is calculated and a normalized anterio–posterior power ratio is found:

$$Q_{\mathrm{APG}} = \frac{P_{\mathrm{ant}}}{P_{\mathrm{ant}} + P_{\mathrm{pos}}}. \tag{3}$$

Here, P_{ant} and P_{pos} represent the mean alpha power over the anterior and posterior regions respectively (see Appendix A.3). Using this ratio, the alpha power gradient is considered within normal range if Q_{APG} is lower than 0.4, moderately differentiated between 0.4 and 0.6, and abnormal or deviant for values above 0.6.

2.3.4. Asymmetries

Asymmetry of the occipital alpha rhythm voltage is present in about 60% of healthy adults (Maulsby et al., 1968). Only 17% of healthy adults show voltage differences larger than 20%, and a mere 1.5% show differences larger than 50% (Maulsby et al., 1968). As a rule therefore, interhemispheric differences in amplitude larger than 50% are considered abnormal (Levin and Lüders, 2000; Maulsby et al., 1968). A significant (>50%) voltage asymmetry of the mu rhythm or temporal alpha activity are often observed in healthy adults; a presence of these findings should therefore be interpreted with caution, as this is common in asymptomatic persons (Ebersole and Pedley, 2003). Frequency asymmetries of 1 Hz or larger also indicate pathology.

Guideline 4: Asymmetrical background patterns are found by comparing rhythmic activity between the two hemispheres in corresponding channel pairs. Reported asymmetries should refer to either *a)* a significant amplitude difference between corresponding channels larger than 50%, or *b)* an abnormal frequency difference (or absence) of rhythmic components in excess of 0.5 Hz (which, for a frequency resolution of 0.5 Hz, indicates a difference of 1 Hz or more).

Automated analysis: Using a Laplacian montage, EEG channels are paired based on symmetrical opposites over the left and right hemispheres:

$$\begin{aligned}\boldsymbol{C}_{\{\mathrm{L,R}\}} = \{&\{Fp1, Fp2\}, \{F7, F8\}, \{F3, F4\}, \{T3, T4\},\\ &\{C3, C4\}, \{T5, T6\}, \{P3, P4\}, \{O1, O2\}\}.\end{aligned} \tag{4}$$

Using the same principle as described by van Putten (2008), a spectral difference is calculated for each channel pair. If the EEG shows spectral asymmetry, it will be reflected in the calculation:

$$Q_{\mathrm{ASYM}}(c_{\{L,R\}}),\ c_{\{L,R\}} \in \boldsymbol{C}_{\{\mathrm{L,R}\}}. \tag{5}$$

In (5), each $c_{\{L,R\}}$ represents one of the channel pairs, and $Q_{\mathrm{ASYM}}(c_{\{L,R\}})$ finds a normalized value to quantify the spectral difference between two channels (see Appendix A.4). Using a threshold of 0.5, the EEG is considered to have an asymmetry for any pair that exceeds that value.

2.3.5. Diffuse slow-wave activity

Diffuse slow-wave activity is hardly present in healthy waking adults (Ebersole and Pedley, 2003). Normal variants exist, although in most cases its presence points to an abnormality that can result from a number of causes. One common cause is diffuse cortical injury such as anoxia (Cloostermans et al., 2011). Slow-wave activity can also be the result of pharmacological effects such as sedatives or anaesthetic medications (San-juan et al., 2010; Blume, 2006).

Guideline 5: Diffuse slow-wave activity results in increased power over the theta and delta bands and decreased power in the alpha and beta bands. Using this as a guideline, the EEG is considered to contain diffuse slow-wave background activity if less than one third of the power in a spectrogram resides above 8 Hz.

Automated analysis: Using the guideline above, the mean spectrum of the EEG is calculated and the power ratio between $P_{\mathrm{low}} = \{2 \ldots 8\}$ Hz and $P_{\mathrm{wide}} = \{2 \ldots 25\}$ Hz is obtained Appendix A.5:

$$Q_{\mathrm{SLOWING}} = P_{\mathrm{low}}/P_{\mathrm{wide}}. \tag{6}$$

For $Q_{\mathrm{SLOWING}} > 0.6$ (i.e., less than 40% of power above 8 Hz), too much slow-wave activity is present and the EEG is categorized as abnormal. EEGs with $Q_{\mathrm{SLOWING}} < 0.6$ are considered to have sufficiently fast rhythmic activity.

2.4. Evaluation

To evaluate the value of the proposed guidelines and quantitative measures, a comparison was made between the described properties from the EEG reports and the interpretations made by automated analysis. As described above and also shown in Table 1, each property was designated by either two or three categories, depending on its relevance. To compare the proposed quantitative measures against visual analysis, three measures were used: sensitivity, specificity, and Fleiss' kappa coefficient (Fleiss, 1971).

Although a common performance measure in quantitative analysis, sensitivity and specificity is defined for two-class problems. It also assumes that the true labels are accurate in describing the property at hand, and does not consider inter- and intra-rater variability. Regardless, these measures can provide valuable information relating to the development of quantitative analysis features. Sensitivity and specificity are calculated for the three properties with a dichotomous outcome: alpha rhythm frequency, reactivity, and the presence or absence of asymmetries.

Given that our goal is to assist the reviewer with analysis of the background pattern, measuring and maximizing the inter-rater agreement between visual and quantitative analysis is of high importantance. Fleiss' kappa coefficient measures inter-rater agreement in properties with multiple outcomes, and is therefore chosen to achieve this.

3. Results

A dataset containing 384 adult EEGs was used to compare the proposed guidelines and automated analysis to visual interpretations. Results from individual properties are provided in succeeding subsections. Table 3 summarizes the agreement for each property, and Section 3.6 gives three examples of how automated analysis can assist in visual interpretation.

3.1. Alpha rhythm frequency

Using *Guideline 1*, substantial agreement ($\kappa = 0.60$) was obtained with visual interpretation in determining if the alpha rhythm frequency was within normal range. The quantitative measure could detect abnormal alpha frequencies with high specificity (0.96), although a lower sensitivity (0.64) was reached. The alpha rhythm could not be identified for 48 of the EEGs with quantitative analysis; either because none was present, or because there was not a significant peak amplitude in the power spectrum. Visual interpretation for these 48 EEGs also ranged from no alpha rhythm observed to a weak but visible peak. The results for alpha rhythm frequency and reactivity in Table 1 and Table 3 only reflect the EEGs in which the rhythm was identified in both visual and quantitative analysis. The mean frequency difference between reported and calculated peak frequencies was 0.42 Hz (SD ±0.66 Hz). The peak frequency reported by visual analysis was often described using a narrow frequency range (mean width 0.57 Hz) instead of

Table 3
Quantitative analysis compared to visual interpretation. Comparisons are made based on automated analysis and the outcome in EEG reports. For properties with a dichotomous outcome, sensitivities and specificities are given in the third and fourth columns. Inter-rater agreement, calculated as kappa coefficients, are shown in the last column.

Background property	Quantity	Sensitivity	Specificity	Inter-rater agreement
Alpha rhythm frequency	Q_{ALPHA}	0.64	0.96	$\kappa = 0.60$
Alpha rhythm reactivity	Q_{REAC}	–	–	$\kappa = 0.34$
Anterio–posterior gradient	Q_{APG}	–	–	$\kappa = 0.19$
Asymmetries	Q_{ASYM}	0.16	0.97	$\kappa = 0.12$
Diffuse slow-wave activity	$Q_{SLOWING}$	0.78	0.98	$\kappa = 0.76$

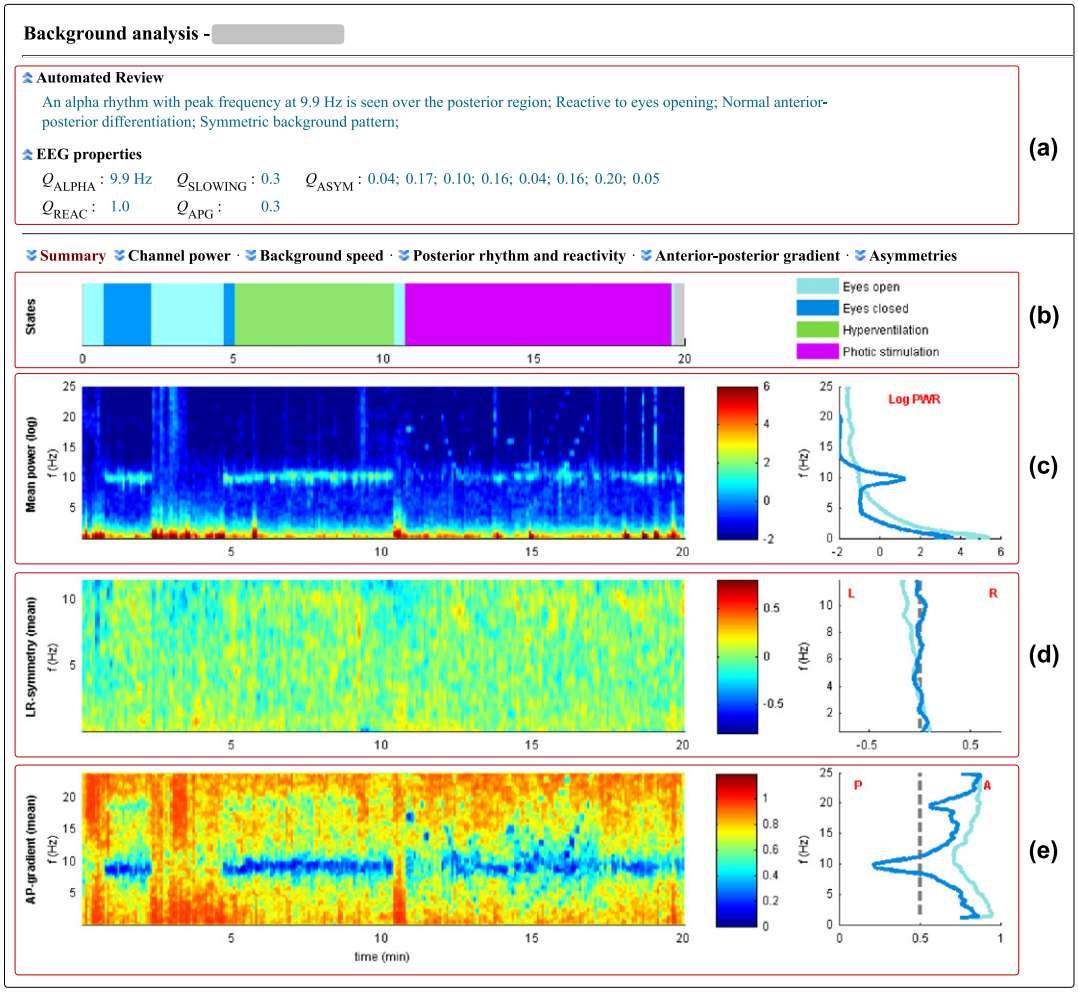

Fig. 1. *Example 1*: An automated EEG report with all background properties described as normal. (a) Quantitative values (Section 2.3) are provided together with an automated free-text description. (b) EEG states (i.e., eyes-open, eyes-closed, hyperventillation etc.) are shown to place quantitative feature plots in correct context. (c) Time-varying spectrum averaged across all channels. (d) Mean left-right symmetry, calculated by averaging Eq. (A.15) over all channels. (e) Time-varying anterio–posterior distribution of rhythmic activity. Note the photic driving responses also visible in (c) and (e).

a single value. In such cases, the frequency difference with quantitative analysis was calculated using the center frequency of that range.

3.2. Alpha rhythm reactivity

Using the calculated peak frequencies, reactivity was calculated for the 336 EEGs with known alpha rhythms. Reactivity of the rhythm after opening or closing the eyes was assigned to one of three categories: substantial, moderate, and low or absent. Using these categories, a fair agreement of $\kappa = 0.34$ was reached.

3.3. Alpha band anterio–posterior gradient

The quantitative measure for an anterio–posterior gradient showed the lowest agreement of all properties with visual interpretation ($\kappa = 0.19$). It should however be noted that it was the most difficult property to categorize from the EEG free text reports due to inconsistent terminology and an unclear border between normal and deviating differentiation.

3.4. Asymmetries

Although it adds significant value to report in which region asymmetries exist, our comparison focussed first on accurately

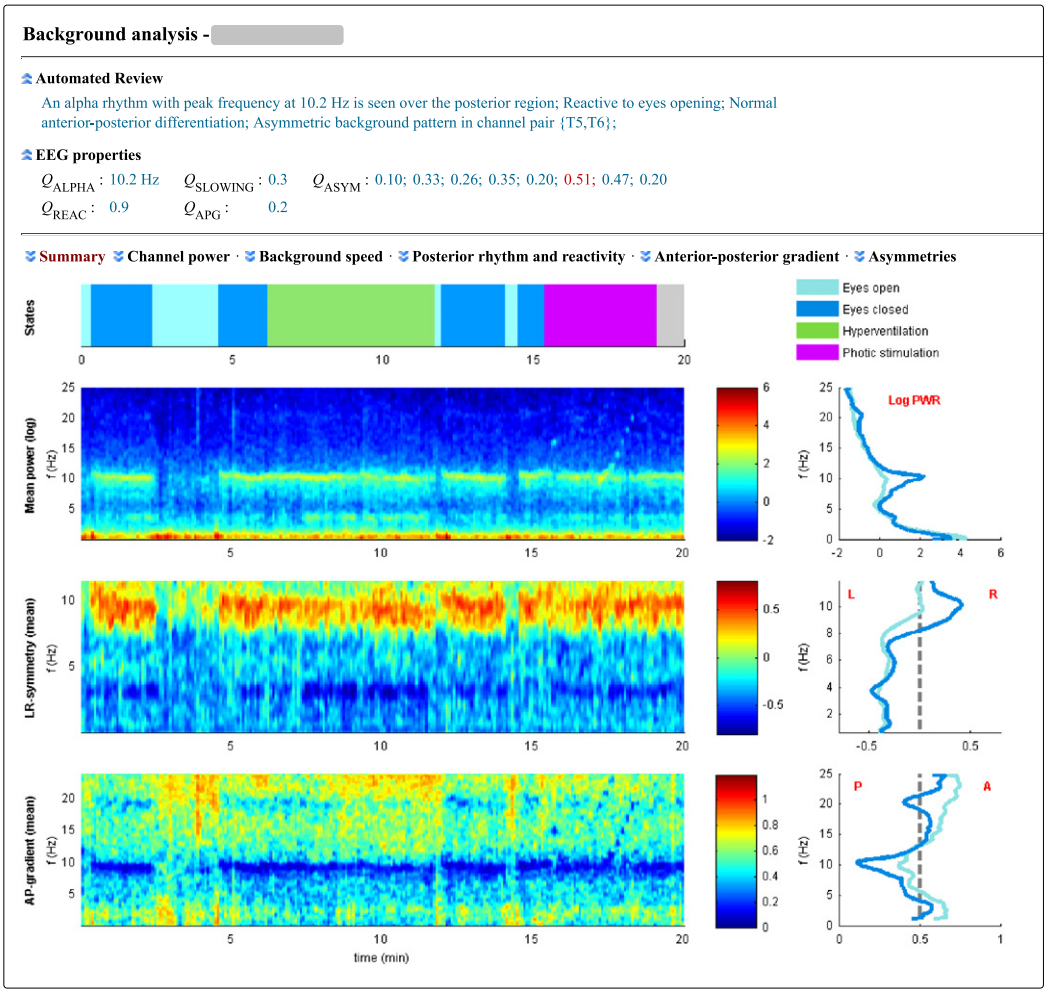

Fig. 2. *Example 2*: An EEG with all background properties described as normal by visual analysis except for asymmetries over temporal and parietal regions. Q_{ASYM} shows two channel pairs above threshold, indicating asymmetries found by quantitative analysis. By looking at the left-right symmetry plot, the asymmetry is also clearly presented to the reviewer in a visual manner.

identifying EEGs with abnormal asymmetries. The agreement between visual interpretation and automated analysis was low ($\kappa = 0.12$). The sensitivity and specificity for this property were 0.16 and 0.97 respectively. No distinction was made between slight and severe asymmetries.

3.5. Diffuse slow-wave activity

To categorize the presence or absence of diffuse slow-wave activity in the background pattern, our algorithm compared the power in the alpha and beta bands to lower bands. As shown in the last row of Table 3, this approach obtained substantial agreement with visual interpretation ($\kappa = 0.76$), high specificity (0.98), and a moderate sensitivity (0.78).

3.6. Automated analysis assisting visual interpretation in practice

Some examples are given to illustrate the added value of automated analysis during an EEG review. Using quantitative analysis performed with the described algorithms, automatically generated reports for three EEGs are presented in Figs. 1–3. At the top of each figure is a summarized outcome of the quantitative analysis written in free text, and below are images to display various EEG properties over time. The images correspond to quantitative features described in Section 2.3, with the exception of not reducing a feature to a single value by averaging over frequency or time. These examples clearly illustrate the added benefit of a quantitative system: outlining the background rhythm of the whole recording on a single page in a clear and simple manner.

For the first example (Fig. 1), an EEG which was considered normal by both visual analysis and quantitative analysis is shown. Fig. 1(b) shows the "assumed" states (i.e., eyes open, eyes close, hyperventilation etc.) of the patient at each time point. This is obtained by parsing the annotations made during recording. By using Fig. 1(b) as context, the reviewer can easily compare changes in properties in the figures below it when switching from states. The second image row, Fig. 1(c), shows a spectrum of the EEG over time, averaged over all channels. Reactivity of the alpha rhythm is clearly visible when comparing the spectrum in Fig. 1(c) to the eyes-open and eyes-closed states in Fig. 1(b). Fig. 1(d) shows the average symmetry over all left-right channel pairs. For this figure, an even symmetry was reported and as seen in the plots, the symmetry appears to be relatively equal. The last row, Fig. 1(e), shows the anterio–posterior distribution of rhythmic activity. As expected for a normal EEG and discussed in Section 2.3.3, higher frequency beta activity is seen most prominently over the frontal regions fading posteriorly, and slower waves (e.g., alpha and mu rhythm) more towards the posterior region.

For the second example (Fig. 2), the EEG background properties were all described as normal, except for a right-dominant alpha

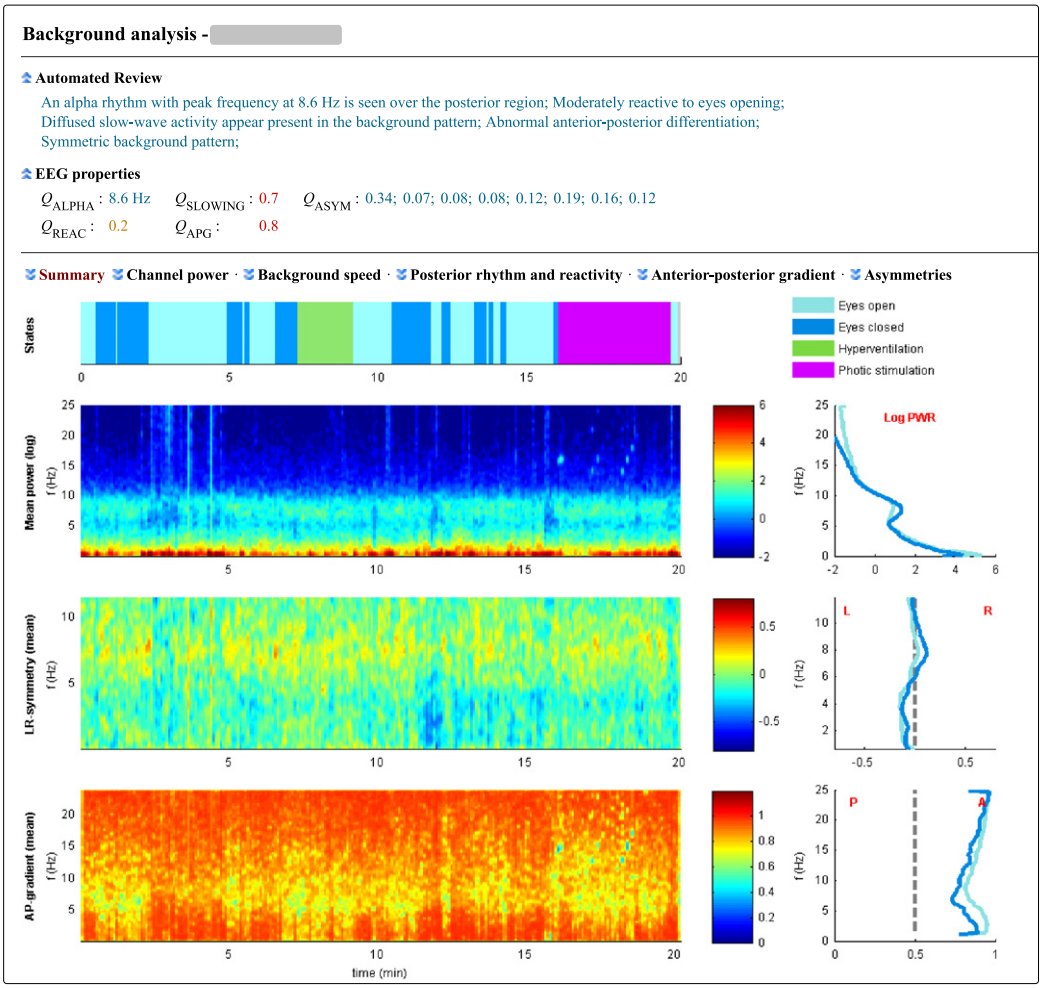

Fig. 3. *Example 3*: An EEG with several abnormalities reported by visual analysis: diffuse slow-wave activity, moderate to low reactivity and an abnormal anterio–posterior gradient. The quantitative features $Q_{SLOWING}$, Q_{REAC}, and Q_{APG} show that automated analysis comes to a similar conclusion. As visual assistance and an outline of the full recording, plots show too much slow-wave activity and no reactivity in the power spectrum between eyes-open and eyes-closed states. Also, an abnormal distribution of rhythmic activity in the bottom row is seen.

asymmetry. This description was based on visual inspection. Quantitative analysis also found all background properties except for asymmetries to be normal. For this EEG, visual inspection and quantitative analysis produced the same outcome. The plots in Fig. 2 also show that all properties appear normal, except for a right-dominant asymmetry in the alpha band and a left-dominant asymmetry in the lower bands.

The third example (Fig. 3) shows an EEG where multiple abnormalities occur. Based on visual inspection, the report described it as containing diffuse slow-wave activity, very low or absent reactivity, and an abnormal anterio–posterior gradient. Automated analysis described the EEG to have diffuse slow-wave activity, moderate reactivity, and an abnormal or deviant anterio–posterior gradient. Once again, the plots in Fig. 3 can assist the reviewer by providing a time-varying summary of the background properties investigated. As an example, compare the fourth row images of Figs. 2 and 3: As expected for normal differentiation in Figs. 1 and 2, rhythms in the alpha and theta bands appear posteriorly, whereas faster rhythms are more visible anteriorly. Fig. 3 however shows that all rhythmic activity appear stronger towards the anterior, corresponding to the EEG report that an abnormal or deviant anterior–posterior gradient exists.

4. Discussion

Current methods of reviewing routine EEGs are based mostly on visual analysis of the raw signals. Although this approach still holds the highest specificity and sensitivity for finding abnormalities, it is time consuming and requires extensive training. Apart from this, visual analysis is susceptible to reviewer bias (Haut et al., 2002; Benbadis et al., 2009; Gerber et al., 2008; Azuma et al., 2003). Automated quantification techniques reduce the time required for reviewing and improve consistency in reporting. They can quantify various properties in EEG and even point out abnormalities if found. However, because external factors (e.g., medication or structural damage) may influence the EEG patterns, final interpretation of the findings is always left to the reviewer.

For quantitative analysis of the background pattern, it is not always easy to define explicit guidelines. Properties such as anterio–posterior gradients, reactivity and asymmetries are well known, but categorizing them as normal, abnormal, or the degree of abnormality, if applicable, is less trivial. Simpler features such as the alpha rhythm frequency and diffused slow-wave activity are better defined, and as shown in Table 3, it becomes easier to find agreement in descriptions. Azuma et al. (2003) showed how inter-rater reliability was improved by having three reviewers agree to use the

same guidelines (Azuma et al., 2003). It is also shown that consistent terminology can improve clarity and enhance sharing capabilities between clinicians, as well as add value to the reporting and querying of data by storing reviews in an organized database (Aurlien et al., 2004).

Our study focusses on quantifying particular key features of the background pattern as a contribution towards improved consistency and inter-rater reliability. Based on the complexity of EEG signals, strict or "narrow" definitions were avoided to prevent a lack of consensus. Instead, an attempt was made to look for simple guidelines that reviewers can follow to improve consistency when discriminating between normal and abnormal behaviour. Five properties were considered as they were the most common in reports related to our study: (i) alpha rhythm peak frequency, (ii) alpha reactivity, (iii) anterio–posterior gradients, (iv) asymmetries, and (v) the presence or absence of diffuse slow-wave activity. For EEGs obtained under other circumstances, e.g., intensive care or emergency units, other properties may have more relevance (Cloostermans et al., 2011; Trevathan and Ellen, 2006; Kurtz et al., 2009).

Previous quantitative analysis studies typically focussed on specialized features to point out a disease or abnormality in the brain (John et al., 1994; Chabot and Serfontein, 1996; Hughes and John, 1999; Bares et al., 2012; Prichep et al., 1994; Calzada-Reyes et al., 2011; Begić et al., 2011; Bjørk et al., 2011; Jiang et al., 2011; Mishra et al., 2011). The difference between these and our study, is that we attempt to quantify the same background properties reported by routine visual analysis, and in addition, compare the quantitative output to that of the human reviewer. To our knowledge, this has not been done before. Our quantitative algorithms made use of the proposed guidelines and required little or no input from the reviewer to perform its analysis. The outcome was compared to reports from visual interpretation, and as shown in Table 3, the agreement between computer-generated features and visual interpretation ranged from slight to substantial. Possible reasons for differences between visual and quantitative analysis can be: (i) a too simplistic nature of the proposed guidelines; (ii) inconsistencies in visual interpretation; (iii) artifacts that interfere with automated analysis; or (iv) the quantitative features may lack full support of the guidelines. Also, the thresholds used to categorize the quantitative features were not optimized, and are merely given to indicate how diagnostic classification can be implemented. With ongoing work, more examples of abnormal background patterns will be collected and further optimization will take place.

This study is a first step, only. We are well aware that the background pattern contains more features than the five discussed in the current contribution, e.g., beta activity, mu- and theta-rhythms, lambda waves or physiological transients such as wicket waves. In addition, we quantify features from adult patients during wakefulness. Therefore, the present computer analysis is far from complete. However, its main purpose is to assist in the visual analysis of the EEG, without an attempt to be a replacement of the human EEG reader. The three examples in Section 3.6 show how the current system already has a practical use in clinical settings, and with an ongoing study we will focus on improving it further.

Given that the evaluation criteria remains constant, automated analysis can reduce inter-rater reliability if used by the reviewer. As also discussed by Anderson and Doolittle (2010), a reviewer will be less likely to trust an algorithm if he does not understand how its values are calculated. It is desirable to keep the logic of the methods clear and transparent. The presented algorithms were designed with a simple and intuitive approach in mind. Some of them were not capable of accurately quantifying an intended property, and improvements are therefore needed to further optimise the system. A common dataset is also needed to construct a gold standard for evaluating new features. As this dataset develops, the guidelines of defining the various properties should also improve.

In summary, current EEG analysis techniques can be improved by supplying reviewers with quantitative measures to assist in the review. In order to increase inter-rater reliability, a consensus is needed to describe EEG properties and to characterize the severity of abnormalities. Five simple guidelines are proposed to describe the EEG background pattern. A quantitative analysis toolkit is developed to describe these properties, and examples show the value added assistance that it can have during a review.

Acknowledgements

The authors would like to extend their gratitude to the reviewers for valuable comments and insights which contributed to this work.

Appendix A. Quantitative features

A.1. Power spectrum

Let $V(c,t)$ be a matrix representing a single EEG with $c = \{1..N\}$ channels over time t. First, the entire EEG is split into smaller segments of 5 s each:

$$W(c,j,t_s) : j \in [1 \ldots M],\ t_s \in [0 \ldots 5], \tag{A.1}$$

with j referring to each segment and t_s to the time in each segment. Using the Welch transform with a 2 s window, zero padded to 2048 sample points and an overlap of 50%, the power spectrum of each segment for each channel is calculated. Let this be represented by

$$P(c,j,f),\ c \in [1 \ldots N],\ j \in [1 \ldots M],\ f \in [f_{\min}, f_{\max}]. \tag{A.2}$$

Each entry in $P(c,j,f)$ contains a discrete Fourier coefficient for channel c, segment j, and at frequency f. The frequency resolution is 0.122 Hz.

A.2. Estimation of the alpha rhythm

A technique described in Lodder and van Putten (2011) was used to find estimates of the alpha rhythm peak frequency in the EEGs. For a full description, refer to the original text.

This technique is based on finding the dominant frequency components between 3 and 18 Hz in localized segments of the EEG. The dominent frequencies are clustered together, and those most persistent during the eyes closed states are considered to represent the alpha rhythm. Given that the alpha rhythm is most prominent over the occipital region, channels $O1$ and $O2$ are used with a common reference montage to estimate the peak frequencies. First, the log spectrum of each segment is calculated:

$$P_{\log}(f) = \log[P(c,j,f)], \quad c \in \{O1, O2\},\ j \in \boldsymbol{J}_{EC}, \tag{A.3}$$

where $\boldsymbol{J}_{EC}$ represents the indices of all segments in the eyes closed state. Then, a curve consisting of two peak components and the power-law background spectrum is fitted to $P_{\log}$:

$$P_{\log}(f) \approx P_{\text{fit}}(f) = P_{\text{pk1}}(f) + P_{\text{pk2}}(f) + P_{\text{bg}}(f), \tag{A.4}$$

$$P_{\text{pk1}}(f) = A_1 \exp\left(\frac{-(f-f_1)^2}{\Delta_1^2}\right), \tag{A.5}$$

$$P_{\text{pk2}}(f) = A_2 \exp\left(\frac{-(f-f_2)^2}{\Delta_2^2}\right), \tag{A.6}$$

$$P_{\text{bg}}(f) = B - C\log(f). \tag{A.7}$$

The peak parameters are used to form clusters based on frequency similarity, and by taking the average of the largest cluster, the alpha rhythm frequency is estimated accordingly.

A.3. Anterio–posterior gradient

Using a Laplacian montage for $P(c,j,f)$, the mean power in the alpha band (8–12 Hz) is calculated as

$$P_{\text{alpha}}(c,j) = \underset{f=\{8\dots12\}\ Hz}{\text{mean}}[P(c,j,f)], \tag{A.8}$$

Segments from the eyes closed state are used to quantify the anterior–posterior gradient. A mean spectrum from these segments are found using

$$P_{EC}(c) = \underset{j\in \boldsymbol{J}_{EC}}{\text{mean}}[P_{\text{alpha}}(c,j)], \tag{A.9}$$

with $\boldsymbol{J}_{EC}$ representing the indices of all segments in the eyes closed state. Using the following channels for the anterior and posterior regions respectively:

$$\boldsymbol{C}_{\text{ant}} = \{Fp1, Fp2, F7, F8, F3, Fz, F4\}, \tag{A.10}$$

$$\boldsymbol{C}_{\text{pos}} = \{T5, T6, P3, P4, Pz, O1, O2\}, \tag{A.11}$$

the mean alpha power over each region is calculated as

$$P_{\text{ant}} = \underset{c\in \boldsymbol{C}_{\text{ant}}}{\text{mean}}[P_{\text{EC}}(c)], \text{ and} \tag{A.12}$$

$$P_{\text{pos}} = \underset{c\in \boldsymbol{C}_{\text{pos}}}{\text{mean}}[P_{\text{EC}}(c)]. \tag{A.13}$$

Following from this, a normalized ratio for the anterior-to-posterior power is found:

$$Q_{\text{APG}} = \frac{P_{\text{ant}}}{P_{\text{ant}} + P_{\text{pos}}}. \tag{A.14}$$

A.4. Asymmetries

Left–right symmetry is calculated by comparing spectral power between the two hemispheres. To increase robustness, power ratios are first calculated in individual segments and then averaged together. Using the channel pairs

$$\boldsymbol{C}_{\{\text{L,R}\}} = \{\{Fp1, Fp2\}, \{F7, F8\}, \{F3, F4\}, \{T3, T4\}, \{C3, C4\}, \{T5, T6\}, \{P3, P4\}, \{O1, O2\}\}, \tag{A.15}$$

a left-right ratio for each pair is calculated:

$$LR(c_{\{L,R\}}, j, f) = \frac{P(c_{\{\text{R}\}}, j, f) - P(c_{\{\text{L}\}}, j, f)}{P(c_{\{\text{R}\}}, j, f) + P(c_{\{\text{L}\}}, j, f)}, \quad c_{\{L,R\}} \in \boldsymbol{C}_{\{\text{L,R}\}}. \tag{A.16}$$

By calculating the mean of all segments:

$$LR_{\text{AVG}}(c_{\{L,R\}}, f) = \left| \underset{j=\{1\dots M\}}{\text{mean}}\,[LR(c_{\{L,R\}}, j, f)] \right|, \tag{A.17}$$

and averaging over $f = \{0.5\dots12\}$ Hz, a single value is obtained to quantify the symmetry for each channel pair:

$$Q_{\text{ASYM}}(c_{\{L,R\}}) = \underset{f=\{0.5\dots12\}\ \text{Hz}}{\text{mean}}[LR_{\text{AVG}}(c_{\{L,R\}}, f)]. \tag{A.18}$$

A.5. Diffused slowing

Diffuse slow-wave activity is detected by finding a ratio in spectral power from a low $\{2\dots8\}$ Hz band to a wider $\{2\dots25\}$ Hz band. Using the common reference montage to calculate $P(c,j,f)$, the following channels are used to find the ratio:

$$\boldsymbol{C}_{\text{SLOWING}} = \{F7, F8, F3, F4, Fz, T3, T4, T5, T6, C3, C4, Cz, P3, P4, Pz, O1, O2\}. \tag{A.19}$$

Using only segments from the eyes closed state, the mean spectrum over all channels are found:

$$P_{EC}(f) = \underset{c\in \boldsymbol{C}_{\text{SLOWING}}}{\text{mean}} \left[\underset{j\in \boldsymbol{J}_{EC}}{\text{mean}}[P(c,j,f)] \right], \tag{A.20}$$

with $\boldsymbol{J}_{EC}$ referring to the indices of all segments in the eyes closed state. The total power in the low and wide spectral bands are calculated:

$$P_{\text{low}} = \sum_{f=2\text{Hz}}^{8\text{Hz}} P_{EC}(f), \tag{A.21}$$

$$P_{\text{wide}} = \sum_{f=2\text{Hz}}^{25\text{Hz}} P_{EC}(f), \tag{A.22}$$

and from these the slowing-ratio is found:

$$Q_{\text{SLOWING}} = P_{\text{low}}/P_{\text{wide}}. \tag{A.23}$$

References

Anderson NR, Doolittle LM. Automated analysis of EEG: Opportunities and pitfalls. J Clin Neurophysiol 2010;27:453–7.

Aurlien H, Gjerde IO, Aarseth JH, Eldøen G, Karlsen B, Skeidsvoll H, et al. EEG background activity described by a large computerized database. Clin Neurophysiol 2004;115:665–73.

Azuma H, Hori S, Nakanishi M, Fujimoto S, Ichikawa N, Furukawa TA. An intervention to improve the interrater reliability of clinical EEG interpretations. Psychiatr Clin Neurosci 2003;57:485–9.

Babiloni C, Vecchio F, Bultrini A, Luca Romani G, Rossini PM. Pre- and poststimulus alpha rhythms are related to conscious visual perception: A high-resolution EEG study. Cerebr Cortex 2006;16:1690–700.

Babiloni C, Lizio R, Vecchio F, Frisoni GB, Pievani M, Geroldi C, et al. Reactivity of cortical alpha rhythms to eye opening in mild cognitive impairment and Alzheimer's disease: An EEG study. J Alzheim Dis 2010;22:1047–64.

Bares M, Novak T, Brunovsky M, Kopecek M, Stopkova P, Krajca V, et al. The change of QEEG prefrontal cordance as a response predictor to antidepressive intervention in bipolar depression. A pilot study. J Psychiatr Res 2012;46:219–25.

Begić D, Popović-Knapić V, Grubišin J, Kosanović-Rajačić B, Filipčić I, Telarović I, et al. Quantitative electroencephalography in schizophrenia and depression. Psychiatr Danub 2011;23:355–62.

Benbadis SR, LaFrance WC, Papandonatos GD, Korabathina K, Lin K, Kraemer HC. Interrater reliability of EEG-video monitoring. Neurology 2009;73:843–6.

Bjørk M, Stovner LJ, Hagen K, Sand T. What initiates a migraine attack? Conclusions from four longitudinal studies of quantitative EEG and steady-state visual-evoked potentials in migraineurs. Acta Neurol Scand Suppl 2011;124:56–63.

Blume WT. Drug effects on EEG. Clin Neurophysiol 2006;23:306–11.

Calzada-Reyes A, Alvarez-Amador A, Galán-García L, Valdés-Sosa M. Electroencephalographic abnormalities in antisocial personality disorder. J Forensic Leg Med 2011;19:29–34.

Chabot RJ, Serfontein G. Quantitative electroencephalographic profiles of children with attention deficit disorder. Biol Psychiatr 1996;40:951–63.

Cloostermans MC, de Vos CC, van Putten MJAM. A novel approach for computer assisted EEG monitoring in the adult ICU. Clin Neurophysiol 2011;122:2100–9.

Douglass LM, Wu JY, Rosman NP, Stafstrom CE. Burst suppression electroencephalogram pattern in the newborn: predicting the outcome. J Child Neurol 2002;17:403–8.

Ebersole JS, Pedley TA. Current practice of clinical electroencephalography. LWW medical book collection. Lippincott Williams & Wilkins; 2003.

Fleiss J. Measuring nominal scale agreement among many raters. Psychol Bull 1971;76:378–82.

Gaál ZA, Boha R, Stam CJ, Molnár M. Age-dependent features of EEG-reactivity-Spectral, complexity, and network characteristics. Neurosci Lett 2010;479:79–84.

Gerber PA, Chapman KE, Chung SS, Drees C, Maganti RK, Ng YT, et al. Interobserver agreement in the interpretation of EEG patterns in critically ill adults. J Clin Neurophysiol 2008;25:241–9.

Halford JJ. Computerized epileptiform transient detection in the scalp electroencephalogram: Obstacles to progress and the example of computerized ECG interpretation. Clin Neurophysiol 2009;120:1909–15.

Haut SR, Berg AT, Shinnar S, Cohen HW, Bazil CW, Sperling MR, et al. Interrater reliability among epilepsy centers: Multicenter study of epilepsy surgery. Epilepsia 2002;43:1396–401.

Hughes JR, John ER. Conventional and quantitative electroencephalography in psychiatry. J Neuropsychiatry 1999;11:190–208.

Ishii R, Canuet L, Kurimoto R, Ikezawa K, Aoki Y, Azechi M, et al. Frontal shift of posterior alpha activity is correlated with cognitive impairment in early Alzheimer's disease: A magnetoencephalography-beamformer study. Psychogeriatrics 2010;10:138–43.

Jiang L, Yin X, Yin C, Zhou S, Dan W, Sun X. Different quantitative EEG alterations induced by TBI among patients with different APOE genotypes. Neurosci Lett 2011;505:160–4.

Jin Y, Potkin SG, Kemp AS, Huerta ST, Alva G, Thai TM, et al. Therapeutic effects of individualized alpha frequency transcranial magnetic stimulation (alphaTMS) on the negative symptoms of schizophrenia. Schizophr Bull 2006;32:556–61.
John ER, Prichep LS, Alper KR, Mas FG, Cancro R, Easton P, et al. Quantitative electrophysiological characteristics and subtyping of schizophrenia. Biol Psychiatr 1994;36:801–26.
Knyazeva MG, Jalili M, Meuli R, Hasler M, De Feo O, Do KQ. Alpha rhythm and hypofrontality in schizophrenia. Acta Psychiatr Scand 2008;118:188–99.
Könönen M, Partanen JV. Blocking of EEG alpha activity during visual performance in healthy adults. A quantitative study. Electroencephalogr Clin Neurophysiol 1993;87:164–6.
Kurtz P, Hanafy KA, Claassen J. Continuous EEG monitoring: Is it ready for prime time? Curr Opin Crit Care 2009;15:99–109.
Lee SH, Park YM, Kim DW, Im CH. Global synchronization index as a biological correlate of cognitive decline in Alzheimer's disease. Neurosci Res 2010;66:333–9.
Levin KH, Lüders H. Comprehensive clinical neurophysiology. W.B. Saunders; 2000.
Lodder SS, van Putten MJAM. Automated EEG analysis: characterizing the posterior dominant rhythm. J Neurosci Meth 2011;200:86–93.
Logi F, Pasqualetti P, Tomaiuolo F. Predict recovery of consciousness in post-acute severe brain injury: the role of EEG reactivity. Brain Inj 2011;25:972–9.
Marcuse LV, Schneider M, Mortati KA, Donnelly KM, Arnedo V, Grant AC. Quantitative analysis of the EEG posterior-dominant rhythm in healthy adolescents. Clin Neurophysiol 2008;119:1778–81.
Maulsby RL, Kellaway P, Graham M. The normative electroencephalographic data reference library. Final report, contract NAS-9-1200 Washington DC National aeronautics and space administration, 1968.
Mishra M, Banday M, Derakhshani R, Croom J, Camarata PJ. A quantitative EEG method for detecting post clamp changes during carotid endarterectomy. J Clin Monit Comput 2011;25:295–308.
Obrist WD. Problems of aging. In: Remond A, editor. Handbook of electroencephalography and clinical neurophysiology. Elsevier Amsterdam; 1976.
Partanen J, Soininen H, Helkala E, Könönen M, Kilpeläinen R, Riekkinen P. Relationship between EEG reactivity and neuropsychological tests in vascular dementia. J Neural Transm 1997;104:905–12.
Prichep LS, John ER, Ferris SH, Reisberg B, Almas M, Alper K, et al. Quantitative EEG correlates of cognitive deterioration in the elderly. Neurobiol Aging 1994;15:85–90.
Ramachandrannair R, Sharma R, Weiss SK, Cortez MA. Reactive EEG patterns in pediatric coma. Pediatr Neurol 2005;33:345–9.
San-juan D, Chiappa KH, Cole AJ. Propofol and the electroencephalogram. Clin Neurophysiol 2010;121:998–1006.
Schomer DL, Lopes da Silva FH. Niedermeyer's Electroencephalography: Basic Principles, Clinical Applications, and Related Fields. Lippincott Williams & Wilkins; 2010.
Segalowitz SJ, Santesso DL, Jetha MK. Electrophysiological changes during adolescence: a review. Brain Cognit 2010;72:86–100.
Segrave RA, Thomson RH, Cooper NR, Croft RJ, Sheppard DM, Fitzgerald PB. Upper alpha activity during working memory processing reflects abnormal inhibition in major depression. J Affect Disord 2010;127:191–8.
Sewards TV, Sewards MA. Alpha-band oscillations in visual cortex: part of the neural correlate of visual awareness? Int J Psychophysiol 1999;32:35–45.
Spronk D, Arns M, Barnett KJ, Cooper NJ, Gordon E. An investigation of EEG, genetic and cognitive markers of treatment response to antidepressant medication in patients with major depressive disorder: a pilot study. J Affect Disord 2011;128:41–8.
Stevens A, Kircher T. Cognitive decline unlike normal aging is associated with alterations of EEG temporo-spatial characteristics. Eur Arch Psychiatr Clin Neurosci 1998;248:259–66.
Trevathan E, Ellen R. Grass lecture: rapid EEG analysis for intensive care decisions in status epilepticus. Am J Electroneurodiagnostic Technol 2006;46:4–17.
van der Hiele K, Vein AA, Reijntjes RHAM, Westendorp RGJ, Bollen ELEM, van Buchem MA, et al. EEG correlates in the spectrum of cognitive decline. Clin Neurophysiol 2007;118:1931–9.
van der Stelt O. Development of human EEG posterior alpha rhythms. Clin Neurophysiol 2008;119:1701–2.
van Putten MJAM. Nearest neighbor phase synchronization as a measure to detect seizure activity from scalp EEG recordings. J Clin Neurophysiol 2003;20:320–5.
van Putten MJAM. The colorful brain: visualization of EEG background patterns. J Clin Neurophysiol 2008;25:63–8.
van Putten MJAM. Essentials of neurophysiology: basic concepts and clinical applications for scientists and engineers 2009;vol. 230. Springer; 2009.
van Putten MJAM, Kind T, Visser F, Lagerburg V. Detecting temporal lobe seizures from scalp EEG recordings: a comparison of various features. Clin Neurophysiol 2005;116:2480–9.
Wilson SB, Emerson R. Spike detection: a review and comparison of algorithms. Clin Neurophysiol 2002;113:1873–81.